Contents

4 Frictional Dynamics **3**
4.1 Equations of motion 5
4.2 Integral properties of the Ekman layer 7
4.3 A bottom boundary layer 10
4.4 A surface boundary layer 15
4.5 Upwelling 27
4.5.1 Coastal Upwelling 27
4.5.2 Equatorial Upwelling 32

Chapter 4

Frictional Dynamics

So far we have dealt with frictionless flows, where the dominant balance is between the Coriolis and pressure gradient forces. That was shown to be a rather good approximation for flows away from boundaries (topography, surface of the ocean, side boundaries, etc.) but this balance does not hold anymore when a boundary is approached, and frictional forces become important. The region where frictional terms have to be taken into account is called a *boundary layer* (see Fig.4.1). Here we will consider the following:

- The boundary layer is Boussinesq.

- The boundary layer has a finite depth, δ, that is less than the total depth of the fluid, H. The depth is given by the level at which frictional stresses vanish. Within the boundary layer, frictional terms are important, whereas geostrophic balance holds beyond it.

- Nonlinear time-dependent terms in the equations of motion are negligible, hydrostasy holds in the vertical, and buoyancy is constant, not varying in the horizontal.

In atmosphere and ocean dynamics, where the focus is on rapidly rotating turbulent fluids, this boundary layer is called *Ekman layer*.

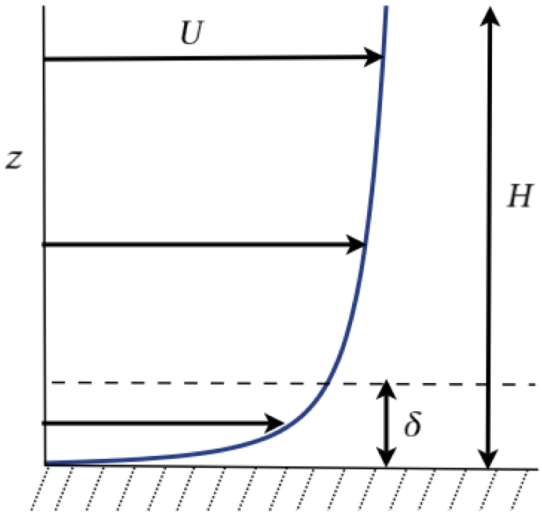

Figure 4.1: *An idealized boundary layer. The boundary layer has thickness δ, within a typical vertical scale H and typical velocity U, which varies rapidly within the boundary layer in order to satisfy the rigid lid boundary condition. [from* **?***]*

The Ekman Layer
The development of the theories for the wind-driven circulation actually has as a foundation the discovery of the so-called Ekman layer and its circulation. In 1898, the polar explorer Nansen observed that icebergs in the Arctic drifted in a direction to the right of the direction of the surface winds, roughly bewteen 20° and 40° to right of the wind stress. This qualitative observation can be explained by the presence of frictional forces. In fact, wind force applied to the surface of the ocean will try to transmit momentum in the same direction. However, as soon as the fluid starts to move, the Coriolis force will come into action deflecting its movement to the right. Importantly, there is also a frictional force within the fluid that will exert some resistance to this movement, and its direction is opposite to the direction of the fluid. The final balance between wind force, Coriolis and frictional forces, will determine the actual direction and velocity of the fluid, which will be to the right of the wind direction in the northern hemisphere.
As we shall see later, Ekman explained quantitatively how the rotation of the earth was responsible for the deflection of the current which Nansen observed.

4.1 Equations of motion

Let us now include frictional effects in our equations of motion

$$\frac{\mathrm{D}u}{\mathrm{D}t} - fv = -\frac{1}{\rho_0}\frac{\partial p}{\partial x} + F_x \tag{4.1}$$

$$\frac{\mathrm{D}v}{\mathrm{D}t} + fu = -\frac{1}{\rho_0}\frac{\partial p}{\partial y} + F_y \tag{4.2}$$

$$\tag{4.3}$$

Here, F_x and F_y are the friction components per unit mass. Assuming no accelerations in the fluid we are left with a balance between three forces

$$-fv = -\frac{1}{\rho_0}\frac{\partial p}{\partial x} + F_x \tag{4.4}$$

$$fu = -\frac{1}{\rho_0}\frac{\partial p}{\partial y} + F_y. \tag{4.5}$$

We can now make progress on the frictional terms. For a geophysical fluid, the vertical component dominates. The Newton's law of friction states that the friction stress $\boldsymbol{\tau}$, which is the force per unit area, is given by

$$\boldsymbol{\tau} = \mu\frac{\partial \mathbf{u}}{\partial z} = \rho_0\nu\frac{\partial \mathbf{u}}{\partial z} = \rho_0 A_z\frac{\partial \mathbf{u}}{\partial z}, \tag{4.6}$$

where μ is the dynamic viscosity and $\nu = \mu/\rho_0$ the kinematic viscosity. For a turbulent fluid such as the ocean, eddy viscosity A_z (coming about from the Reynolds stresses $-\overline{u'w'} = A_z\partial u/\partial z$) has a value $\sim 10^{-1}$ m^2 s^{-1}.

The eddy friction stress can be expressed in terms of a mass of fluid, where for the vertical component leads to frictional force per unit mass

$$\frac{1}{\rho_0}\frac{\partial \tau}{\partial z} = \frac{1}{\rho_0}\frac{\partial}{\partial z}\left(\rho_0 A_z\frac{\partial u}{\partial z}\right) = A_z\frac{\partial^2 u}{\partial z^2}. \tag{4.7}$$

Our equations of motion thus reduce to

$$-fv = -\frac{1}{\rho_0}\frac{\partial p}{\partial x} + A_z\frac{\partial^2 u}{\partial z^2} \tag{4.8}$$

$$fu = -\frac{1}{\rho_0}\frac{\partial p}{\partial y} + A_z\frac{\partial^2 v}{\partial z^2}. \tag{4.9}$$

Or simply

$$\boxed{\mathbf{f}\times\mathbf{u} = -\frac{1}{\rho_0}\nabla_z p + A\frac{\partial^2 \mathbf{u}}{\partial z^2}}. \tag{4.10}$$

where $\mathbf{f} = f\mathbf{k}$. The momentum equation in the vertical is the hydrostatic balance, and the set is completed with mass continuity, $\nabla\cdot\mathbf{u} = 0$.

The Ekman number

We now apply the usual scaling arguments to the equations and obtain the Ekman number

$$\mathrm{Ek} = \left(\frac{A}{f_0 H^2}\right), \tag{4.11}$$

which determines the importance of frictional terms in the horizontal equations. For interior flows, $Ek < 1$, and the flow is geostrophic. Within the Ekman layer, $Ek \geq 1$, and friction is important. The difference between the geostrophic equations and the equations of motion when frictional effects are retained is thus clear.

This implies that the vertical velocities w are not negligible within the boundary layer, near the sea surface and bottom. Friction terms are small enough to be neglected only in the interior of the ocean. If we do not neglect the friction term in the momentum equation this means that the friction term is comparable in size to the Coriolis term

$$A_z \frac{\partial^2 u}{\partial z^2} \simeq f u \tag{4.12}$$

A scaling analysis reveals that

$$A_z (U/H^2) \simeq f U \tag{4.13}$$

For typical values $A_z = 10^{-1}$ m^2 s^{-1} and $f = 10^{-4} s^{-1}$ we get

$$H^2 \simeq \frac{A_z U}{f U} = 10^{-1}/10^{-4} = 10^3 \mathrm{m}^2. \tag{4.14}$$

A typical boundary layer is in the order of $H \simeq 30$ m and frictional effects can be felt up to a 100 m or so.

Momentum balance

We write the velocity field and the pressure field as the sum of interior geostrophic part and a boundary layer correction:

$$\mathbf{u} = \mathbf{u_g} + \mathbf{u_E}, \qquad p = p_g + p_E, \tag{4.15}$$

where the Ekman layer corrections are negligible away from the boundary layer. In the fluid interior we have, by hydrostatic balance, $\frac{\partial p_g}{\partial z} = 0$, because we have considered the fluid to have constant buoyancy $b = -g\rho'/\rho_0$. In the boundary layer, we still have $\frac{\partial p_g}{\partial z} = 0$ and, to satisfy

hydrostasy, $\frac{\partial p_E}{\partial z} = 0$. But because p_E vanishes away from the boundary, $p_E = 0$ everywhere. This implies that there is no boundary layer in the pressure field. For the Ekman layer then, the horizontal momentum equation becomes

$$\mathbf{f} \times \mathbf{u_E} = A_z \frac{\partial^2 \mathbf{u_E}}{\partial z^2}, \tag{4.16}$$

the dominant force balance in the Ekman layer is thus between the Coriolis force and friction.

We can now estimate the depth over which the Ekman layer extends. Recalling the Ekman number:

$$\mathrm{Ek} = \frac{A_z}{\Omega d^2} \simeq 1, \tag{4.17}$$

this implies that $d = (A_z/\Omega)^{1/2}$. With typical values $A = 10^{-1}$ m^2 s^{-1} and $\Omega = 10^{-4}$ s^{-1}, we get a boundary layer of the order of 30 m.

4.2 Integral properties of the Ekman layer

Let's now deduce the properties of the Ekman layer without specifying the frictional stress tensor τ_{ij}.

The Ekman mass transport

The frictional-geostrophic balance is

$$\mathbf{f} \times \mathbf{u} = -\frac{1}{\rho_0} \nabla_z p + \frac{1}{\rho_0} \frac{\partial \boldsymbol{\tau}}{\partial z}, \tag{4.18}$$

where $\boldsymbol{\tau}$ is zero at the edge of the Ekman layer. In the Ekman layer we have

$$\mathbf{f} \times \mathbf{u_E} = \frac{1}{\rho_0} \frac{\partial \boldsymbol{\tau}}{\partial z}. \tag{4.19}$$

As we seek properties for the entire boundary layer, let's integrate over its thickness

$$\mathbf{f} \times \int_{Ek} \rho_0 \mathbf{u_E} \, \mathrm{d}z = \boldsymbol{\tau}_T - \boldsymbol{\tau}_B, \tag{4.20}$$

where subscripts T and B are for the stresses at the top and bottom of the Ekman boundary layer.

We now define the ageostrophic mass transport in the Ekman layer as

$$\mathbf{M}_E = \int_{Ek} \rho_0 \mathbf{u_E} \, \mathrm{d}z. \tag{4.21}$$

For a bottom Ekman layer, stress at the top will be zero. For a top Ekman layer, stress at the bottom will be zero:

$$Top: \quad \mathbf{f} \times \mathbf{M}_E = \boldsymbol{\tau}_T \tag{4.22}$$

$$Bottom: \quad \mathbf{f} \times \mathbf{M}_E = -\boldsymbol{\tau}_B \tag{4.23}$$

which is equivalent to writing

$$\boxed{Top: \quad \mathbf{M}_E = -\frac{1}{f}\,\mathbf{k} \times \boldsymbol{\tau}_T} \tag{4.24}$$

$$\boxed{Bottom: \quad \mathbf{M}_E = \frac{1}{f}\,\mathbf{k} \times \boldsymbol{\tau}_B.} \tag{4.25}$$

Take a situation in which $\tau_x = 0$ and therefore $M_E^y = \int_{Ek} \rho_0 v_E \, \mathrm{d}z = 0$ but $M_E^x > 0$ with $\tau^y > 0$. **The net transport is thus at right angles to the stress at the surface (to the right for $f > 0$), and proportional to the magnitude of the stress.**

Integrated over the depth of the Ekman layer, the surface stress must be balanced by the Coriolis force, which in turn acts at right angles to the mass transport. **Mass transports in a top oceanic and bottom atmospheric Ekman layers are equal and opposite, because the stress is continuous across the ocean-atmosphere interface (see Fig.4.12).**

The Ekman vertical velocity: Ekman Pumping

We now obtain an expression for the vertical velocity induced by an Ekman layer. We start from the mass conservation equation

$$\frac{\partial u}{\partial x} + \frac{\partial v}{\partial y} + \frac{\partial w}{\partial z} = 0 \tag{4.26}$$

and we integrate this over the Ekman layer

$$\int_{Ek} \Big(\frac{\partial u}{\partial x} + \frac{\partial v}{\partial y} \Big) \mathrm{d}z = -\int_{Ek} \frac{\partial w}{\partial z} \mathrm{d}z. \tag{4.27}$$

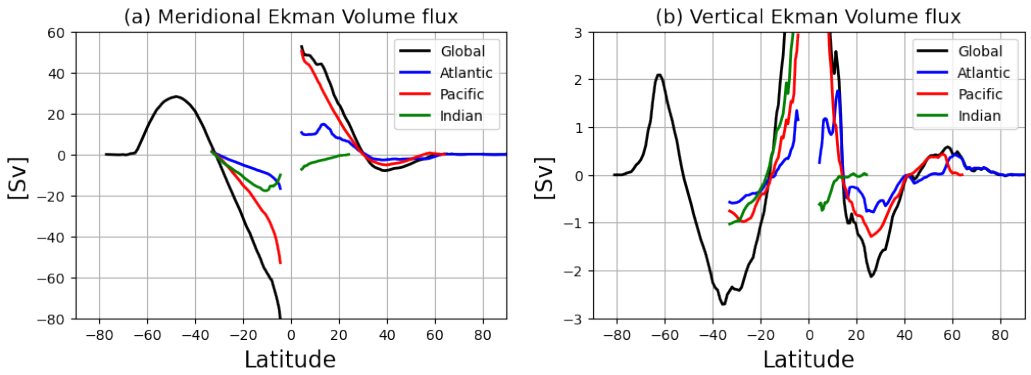

Figure 4.2: *(a) Meridional Ekman volume flux, -$\tau^x/(f\rho_0)$, for each of the world oceans as a function of latitude. Note the maximum of V_E at about 45°N and the changeover between westerlies and easterlies at about 30°N. (b) Vertical Ekman volume flux, w_e, for the world's oceans (see also* **?**).

Remembering that we have defined $\mathbf{M}_E = \int_{Ek} \rho_0 \mathbf{u_E}\, \mathrm{d}z$,

$$\frac{1}{\rho_0} \nabla \cdot \mathbf{M}_E = -\int_{Ek} \frac{\partial w}{\partial z} \mathrm{d}z \tag{4.28}$$

$$\frac{1}{\rho_0} \nabla \cdot \mathbf{M}_E = -(w_T - w_B). \tag{4.29}$$

Using Eq.4.20:

$$\mathbf{f} \times \mathbf{M}_E = \boldsymbol{\tau}_T - \boldsymbol{\tau}_B, \tag{4.30}$$

and taking its curl we find

$$\nabla \cdot \mathbf{M}_E = \mathrm{curl}_z[(\boldsymbol{\tau}_T - \boldsymbol{\tau}_B)/f] \tag{4.31}$$

where we have used the curl_z operator on a vector $\mathbf{A}$ defined as $\mathrm{curl}_z \mathbf{A} \equiv \partial_x A_y - \partial_y A_x$.

We now make use of Eq.4.29 and we obtain

$$\frac{1}{\rho_0} \nabla \cdot \mathbf{M}_E = -(w_T - w_B) = \frac{1}{\rho_0} \mathrm{curl}_z[(\boldsymbol{\tau}_T - \boldsymbol{\tau}_B)/f]. \tag{4.32}$$

For a top Ekman layer we have:

$$\boxed{w_B = \frac{1}{\rho_0} \mathrm{curl}_z\left(\boldsymbol{\tau}_T/f\right)} \tag{4.33}$$

For a bottom Ekman layer we have:

$$\boxed{w_T = \frac{1}{\rho_0}\,\mathrm{curl}_z\Big(\boldsymbol{\tau}_B/f\Big)} \tag{4.34}$$

Friction induces a vertical velocity in the Ekman layer, proportional to the curl of the stress at the surface. This vertical velocity is called *Ekman pumping* (see Fig.4.2). The production of a vertical velocity at the edge of the Ekman layer is one of the most important effects of the layer, especially with regard to the large-scale circulation, for it provides an efficient means whereby surface fluxes are communicated to the interior flow.

4.3 A bottom boundary layer

We now derive the properties for the bottom boundary layer. If you are more atmospherically inclined, think of this bottom boundary layer as the one generated by the wind over some topography.

Our momentum equations (Eq.4.10) are completed by the mass conservation equation

$$\frac{\partial u}{\partial x} + \frac{\partial v}{\partial y} + \frac{\partial w}{\partial z} = 0 \tag{4.35}$$

and hydrostatic balance in the vertical

$$0 = -\frac{1}{\rho_0}\frac{\partial p}{\partial z}. \tag{4.36}$$

Remember we are in a Boussinesq fluid. The flow can be divided into an interior geostrophic part

$$-fv_g = -\frac{1}{\rho_0}\frac{\partial p}{\partial x} \tag{4.37}$$

$$fu_g = -\frac{1}{\rho_0}\frac{\partial p}{\partial y}, \tag{4.38}$$

$$\tag{4.39}$$

or

$$f(u_g, v_g) = (-\frac{\partial \phi}{\partial y}, \frac{\partial \phi}{\partial x}) \tag{4.40}$$

where $\phi \equiv p/\rho_0$. And a boundary layer correction

$$-fv = -\frac{1}{\rho_0}\frac{\partial p}{\partial x} + A\frac{\partial^2 u}{\partial z^2} \tag{4.41}$$

$$fu = -\frac{1}{\rho_0}\frac{\partial p}{\partial y} + A\frac{\partial^2 v}{\partial z^2}. \tag{4.42}$$

$$\tag{4.43}$$

Given Eq.4.40, the frictional-geostrophic balance can be written as

$$-f(v - v_g) = A\frac{\partial^2 u}{\partial z^2} \tag{4.44}$$

$$f(u - u_g) = A\frac{\partial^2 v}{\partial z^2}, \tag{4.45}$$

or even better as

$$\mathbf{f} \times (\mathbf{u} - \mathbf{u_g}) = A\frac{\partial^2 \mathbf{u}}{\partial z^2}. \tag{4.46}$$

Our boundary conditions will be

$$\text{at z=0:} \quad u = 0, v = 0 \quad \text{(no slip boundary condition)} \tag{4.47}$$

$$\text{as z}\rightarrow\infty\text{:} \quad u = u_g, v = v_g \quad \text{(a geostrophic interior).} \tag{4.48}$$

We seek solutions of the form

$$u = u_g + A_0 e^{\alpha z}, \quad v = v_g + B_0 e^{\alpha z}, \tag{4.49}$$

where A_0 and B_0 are constants. Substituting into Eq.4.46 leads to

$$fA_0 - AB_0\alpha^2 = 0, \quad -fB_0 - AA_0\alpha^2 = 0. \tag{4.50}$$

Remember that, given the absence of temperature horizontal gradients, via thermal wind, $\partial_z u_g = \partial_z v_g = 0$.

For non-trivial solutions we have $\alpha^4 = -f^2/A^2$, from which we find $\alpha = \pm(1 \pm i)(1/d)$, where $d = (2A/f)^{1/2}$. Using the boundary conditions we obtain the solution

$$u = u_g - e^{-z/d}\Big[u_g cos(z/d) + v_g sin(z/d)\Big] \tag{4.51}$$

$$v = v_g + e^{-z/d}\Big[u_g sin(z/d) - v_g cos(z/d)\Big]. \tag{4.52}$$

We have used $d = (2A/f)^{1/2}$, the depth of the Ekman layer. It is apparent that the solution decays exponentially from the surface with an e-folding scale equal to d.

Now let's suppose a flow that is directed eastward and has zero meridional component ($u_g > 0$, $v_g = 0$). Velocities reduce to

$$u = u_g[1 - e^{-z/d}cos(z/d)] \tag{4.53}$$
$$v = u_g \quad e^{-z/d}sin(z/d). \tag{4.54}$$

This is already telling us that the meridional velocity within the boundary layer is not zero. As $z \to 0$[1] we have

$$u = u_g[1 - (1 - z/d)] = u_g z/d \tag{4.55}$$
$$v = u_g \quad (1 - z/d)z/d = u_g z/d - \cancelto{0}{u_g z^2/d^2}. \tag{4.56}$$

Hence, u and v are equal and generate a flow that is 45° to the left of the direction of the interior flow (to the right when $f < 0$).

We can find a local maximum for the velocity in the boundary layer

$$\frac{\partial u}{\partial z} = 0 \to \partial_z[u_g - u_g e^{-z/d}cos(z/d)] = 0 \tag{4.57}$$

$$\frac{1}{d}u_g e^{-z/d}cos(z/d) + \frac{1}{d}u_g e^{-z/d}sin(z/d) = 0$$
$$cos(z/d) + sin(z/d) = 0$$
$$tan(z/d) = -1$$

And so the depth of maximum velocity is

$$z = \frac{3\pi}{4}d.$$

At this depth

$$u = u_g\Big(1 - e^{\frac{3\pi}{4}}cos(\frac{3\pi}{4})\Big) = 1.07u_g. \tag{4.58}$$

Hence, the theoretical value of u reaches values larger then the interior geostrophic flow because of frictional effects and redistribution of momentum within the boundary layer.

The bottom Ekman layer can be seen in Fig.4.3, where the Ekman spiral is depicted. At the bottom, the flow is at 45° to the left of the interior geostrophic flow. The maximum u is obtained at $z/d = \frac{3\pi}{4}$

[1]Taylor expanding and neglecting higher order terms $e^{-z/d} = 1 - z/d + \cancel{z^2/(2d^2)}$; $cos(z/d) = 1 - \cancel{z^2/(2d^2)}$; $sin(z/d) = z/d - \cancel{z^3/(3d^3)}$

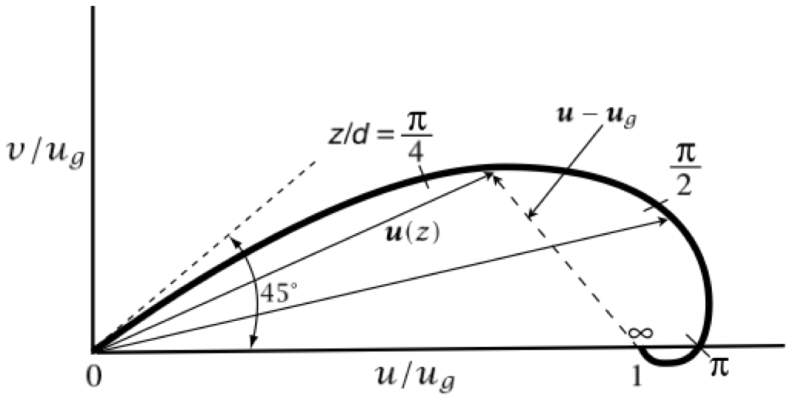

Figure 4.3: *The idealized Ekman layer solution at the bottom for $v_g = 0$. [from* **?***]*

Transport and vertical velocity

We now find an expression for the (cross-isobaric) transport produced by frictional effects. For $v_g = 0$, we have

$$V = \int_0^\infty v \, \mathrm{d}z = \int_0^\infty u_g e^{-z/d} sin(z/d) \, \mathrm{d}z = \frac{d}{2} u_g \quad (4.59)$$

$$U = \int_0^\infty (u - u_g) \, \mathrm{d}z = -\int_0^\infty u_g e^{-z/d} sin(z/d) \, \mathrm{d}z = -\frac{d}{2} u_g, \quad (4.60)$$

and the general case with $v_g \neq 0$ is simply

$$V = \frac{d}{2}(u_g - v_g) \quad (4.61)$$

$$U = -\frac{d}{2}(u_g + v_g). \quad (4.62)$$

The total mass transport caused by frictional forces is thus

$$\mathbf{M}_E = \frac{\rho_0 d}{2}\Big[-\mathbf{i}(u_g + v_g) + \mathbf{j}(u_g - v_g)\Big]. \quad (4.63)$$

Recalling that the frictionally induced transport in the Ekman layer is related to the stress at the surface by $\mathbf{M}_E = (\mathbf{k} \times \boldsymbol{\tau}_B)/f$, a full picture of stress, cross-isobaric velocity and total transport is given in Fig.4.4.

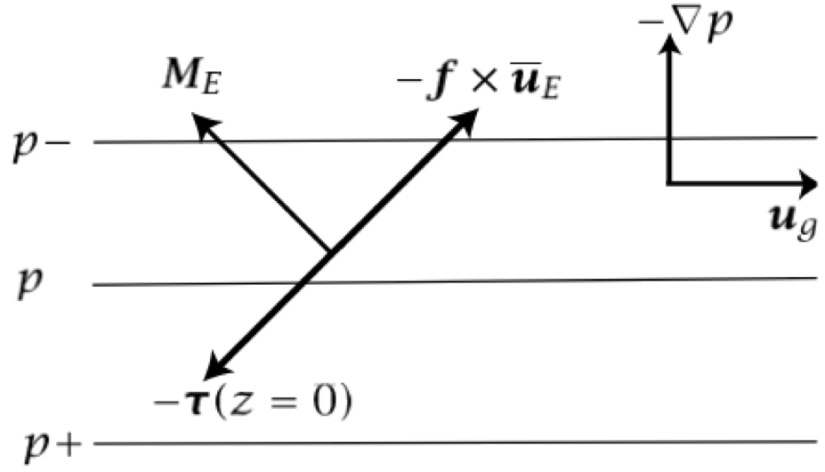

Figure 4.4: *A bottom Ekman layer, generated from an eastward geostrophic flow above. An overbar denotes a vertical integral over the Ekman layer. so that* $-f \times \overline{u}_E$ *is the Coriolis force on the vertically integrated Ekman velocity.* $\mathbf{M}_E$ *is the frictionally induced boundary layer transport, and* $\boldsymbol{\tau}$ *is the stress. [from* **?***]*

The flow within the Ekman layer has a nonzero divergence, indeed:

$$\frac{\partial U}{\partial x} + \frac{\partial V}{\partial y} = -\frac{d}{2}\Big[\partial_x(u_g + v_g) - \partial_y(u_g - v_g)\Big] \tag{4.64}$$

$$= \frac{d}{2}\Big[-(\partial_x u_g + \partial_y v_g) - \partial_x v_g + \partial_y u_g\Big]. \tag{4.65}$$

The first term on the r.h.s. is zero because the interior flow is non-divergent, hence:

$$\frac{\partial U}{\partial x} + \frac{\partial V}{\partial y} = -\frac{d}{2}(\partial_x v_g - \partial_y u_g) = -\frac{d}{2}\zeta_g \tag{4.66}$$

The vertical velocity at the top of the Ekman layer is, for a constant f (and using Eq.4.34)

$$\boxed{w_E = -\frac{1}{\rho_0}\nabla \cdot \boldsymbol{M}_E = \frac{1}{\rho_0}\,\mathrm{curl}_z\Big(\boldsymbol{\tau}_B/f\Big) = \frac{d}{2}\zeta_g} \tag{4.67}$$

There will be divergence if the interior geostrophic flow presents vorticity. **The vertical velocity at the top of the bottom Ekman layer, which**

arises because of the frictionally-induced divergence of the flow in the Ekman layer, is proportional to the geostrophic vorticity and to the Ekman layer height.

4.4 A surface boundary layer

We now look for solutions for a surface Ekman layer. In this case, the wind provides a stress on the upper ocean, and the Ekman layer serves to communicate this to the ocean interior.

We start again with our momentum equations, which for the interior geostrophic flow are

$$-fv_g = -\frac{1}{\rho_0}\frac{\partial p}{\partial x} \tag{4.68}$$

$$fu_g = -\frac{1}{\rho_0}\frac{\partial p}{\partial y}, \tag{4.69}$$

or

$$f(u_g, v_g) = (-\frac{\partial \phi}{\partial y}, \frac{\partial \phi}{\partial x}) \tag{4.70}$$

where $\phi \equiv p/\rho_0$. And for the Ekman layer

$$-fv = -\frac{1}{\rho_0}\frac{\partial p}{\partial x} + A\frac{\partial^2 u}{\partial z^2} \tag{4.71}$$

$$fu = -\frac{1}{\rho_0}\frac{\partial p}{\partial y} + A\frac{\partial^2 v}{\partial z^2}. \tag{4.72}$$

$$\tag{4.73}$$

The frictional-geostrophic balance can be written again as

$$-f(v - v_g) = A\frac{\partial^2 u}{\partial z^2} \tag{4.74}$$

$$f(u - u_g) = A\frac{\partial^2 v}{\partial z^2}, \tag{4.75}$$

or even better as

$$\boxed{\mathbf{f} \times (\mathbf{u} - \mathbf{u_g}) = A\frac{\partial^2 \mathbf{u}}{\partial z^2}} \tag{4.76}$$

Our boundary conditions will be

$$\text{at z=0:} \qquad \tau^x = \rho_0 A \frac{\partial^2 u}{\partial z^2}, \text{ (a given surface stress)} \tag{4.77}$$

$$\tau^y = \rho_0 A \frac{\partial^2 v}{\partial z^2} \tag{4.78}$$

$$\text{as z}\rightarrow -\infty: \qquad u = u_g \text{ (a geostrophic interior)} \tag{4.79}$$

$$v = v_g \tag{4.80}$$

We now introduce the kinematic wind stress at the surface, $\tilde{\boldsymbol{\tau}} = \boldsymbol{\tau}/\rho_0$, and seek solutions by the same method we used for the bottom layer:

$$u = u_g + \frac{\sqrt{2}}{fd} e^{z/d} \Big[\tilde{\tau}^x cos(z/d - \pi/4) - \tilde{\tau}^y sin(z/d - \pi/4) \Big], \tag{4.81}$$

$$v = v_g + \frac{\sqrt{2}}{fd} e^{z/d} \Big[\tilde{\tau}^x sin(z/d - \pi/4) + \tilde{\tau}^y cos(z/d - \pi/4) \Big]. \tag{4.82}$$

Note that the boundary layer correction depends only on the imposed surface stress, and not on the interior flow. In the absence of an imposed stress the boundary layer correction is zero, and $\mathbf{u} = \mathbf{u}_g$. Similar to the bottom boundary layer, the velocity vector traces a diminishing spiral as it descend into the interior (Fig.4.5). The velocity within the boundary depends on its depth, $d = \sqrt{\frac{2A}{f}}$, which depends on the eddy viscosity A. If the fluid is not very viscous, it will generate a small Ekman layer, and the velocity within the layer can be large for small stresses.

What is the value and direction of the surface velocity? at $z = 0$ we have

$$u(0) = u_g + \frac{\sqrt{2}}{fd} \Big[\tilde{\tau}^x cos(-\pi/4) - \tilde{\tau}^y sin(-\pi/4) \Big], \tag{4.83}$$

$$v(0) = v_g + \frac{\sqrt{2}}{fd} \Big[\tilde{\tau}^x sin(-\pi/4) + \tilde{\tau}^y cos(-\pi/4) \Big]. \tag{4.84}$$

Since $cos(-\pi/4) = \sqrt{2}/2$ and $sin(-\pi/4) = -\sqrt{2}/2$, the solution is

$$u(0) = u_g + \frac{\sqrt{2}}{fd} \Big[\tilde{\tau}^x \frac{\sqrt{2}}{2} + \tilde{\tau}^y \frac{\sqrt{2}}{2} \Big], \tag{4.85}$$

$$v(0) = v_g + \frac{\sqrt{2}}{fd} \Big[- \tilde{\tau}^x \frac{\sqrt{2}}{2} + \tilde{\tau}^y \frac{\sqrt{2}}{2} \Big]. \tag{4.86}$$

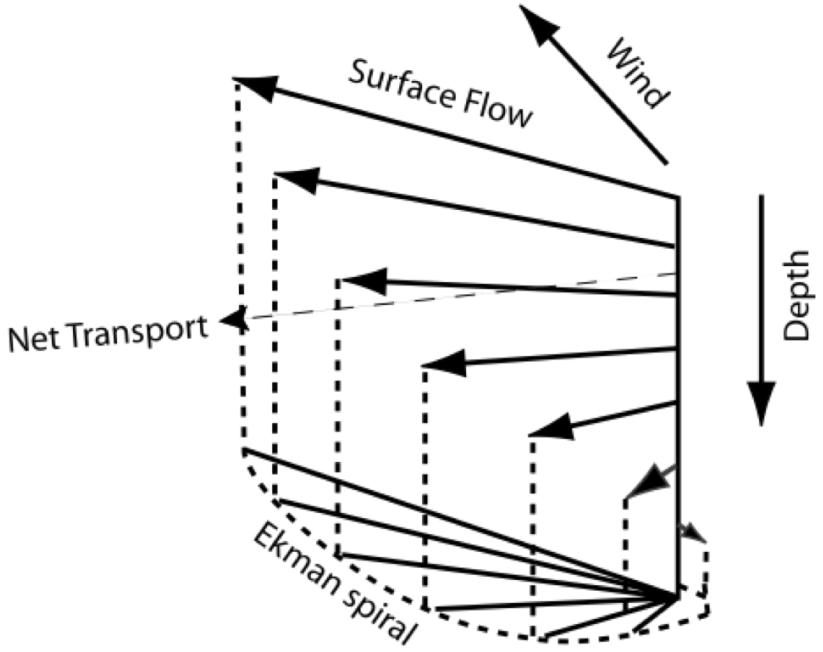

Figure 4.5: *An idealized Ekman spiral in the southern hemisphere ocean, driven by an imposed wind stress. The net transport is at right angles to the wind, independent of the detailed form of the friction. The angle of the surface flow is at 45° to the wind (only for a Newtonian viscosity). [from* **?***]*

Suppose the surface wind is eastward. In this case $\tilde{\tau}^y = 0$ and the solutions reduce to

$$u(0) = u_g + \frac{\sqrt{2}}{fd}\left[\tilde{\tau}^x \frac{\sqrt{2}}{2}\right], \tag{4.87}$$

$$v(0) = v_g - \frac{\sqrt{2}}{fd}\left[\tilde{\tau}^x \frac{\sqrt{2}}{2}\right]. \tag{4.88}$$

The velocity at the surface of the Ekman layer are simply

$$u(0) - u_g = \frac{\tilde{\tau}^x}{fd}, \tag{4.89}$$

$$v(0) - v_g = -\frac{\tilde{\tau}^x}{fd}. \tag{4.90}$$

Therefore the magnitudes of the frictional flow in the x and y directions are equal to each other, and the ageostrophic flow is 45° to the right (for $f > 0$**) of the wind.** This result does not depend on the size of the viscosity.

Transport and vertical velocity (or Ekman pumping / suction)

The transport induced by the surface stress is obtained by integrating (4.81) and (4.82)

$$U = \int_{-\infty}^{0} (u - u_g)\,\mathrm{d}z = \frac{\tilde{\tau}^y}{f} \tag{4.91}$$

$$V = \int_{-\infty}^{0} (v - v_g)\,\mathrm{d}z = -\frac{\tilde{\tau}^x}{f}, \tag{4.92}$$

which indicates that **the ageostrophic transport is perpendicular to the wind stress**, as previously noted (see Fig.4.6). It should be noted that these results are correct even if the details of the Ekman spiral are not.

Again the ageostrophic flow will be divergent

$$\int_{-\infty}^{0} \mathrm{d}z\left(\frac{\partial U}{\partial x} + \frac{\partial V}{\partial y}\right) = \frac{1}{f}\left(\partial_x \tilde{\tau}^y - \partial_y \tilde{\tau}^x\right) = \tag{4.93}$$

$$w_E = \frac{1}{f}\,\mathrm{curl}_z \tilde{\boldsymbol{\tau}}. \tag{4.94}$$

As previously noted in (4.33). At the edge of the Ekman layer the vertical velocity (*Ekman pumping*) is proportional to the curl of the wind stress.

The Ekman pumping is associated with the frictionally induced vertical velocity w_E. This vertical Ekman velocity starts with zero due to

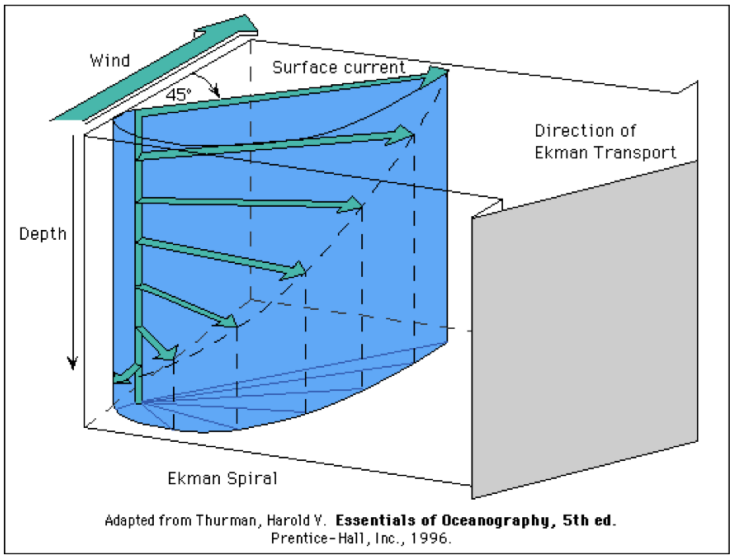

Figure 4.6: An idealized Ekman velocity spiral.

the boundary condition at the surface, followed by an exponential pattern within the top Ekman layer, and approaches a constant below.

It is quite hard to observe Ekman spirals both in the ocean and atmosphere (but not in a laboratory where you can control viscosity and background conditions!). The theory does not take into account stratification, gravity waves and assumes a steady wind. Nevertheless both the Ekman mass transport and vertical velocity are independent of details of the Ekman layer, and only depend on the imposed stress (Fig. 4.7 and Fig. 4.10).

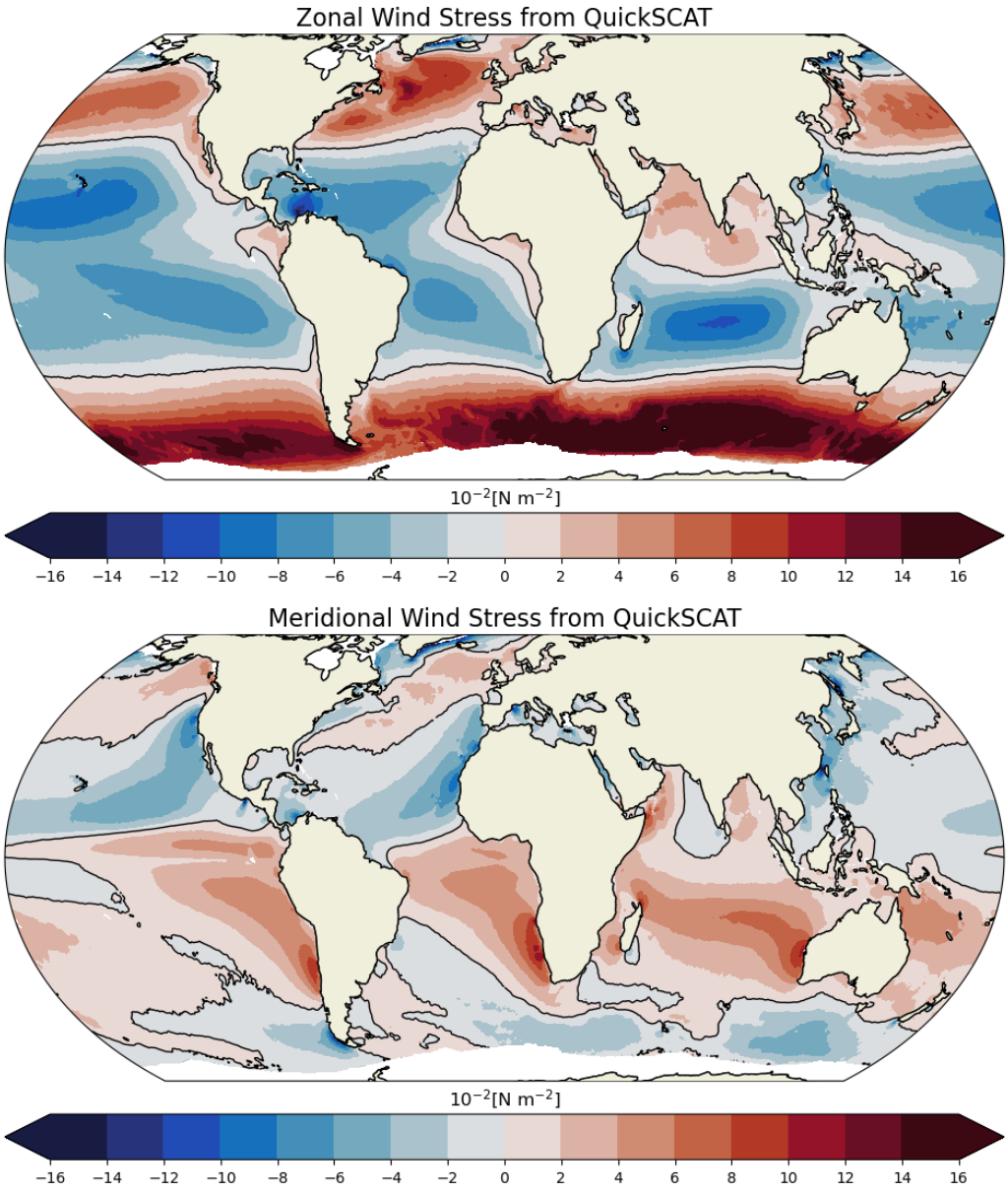

Figure 4.7: *Climatological zonal and meridional wind stress from QuickSCAT.*

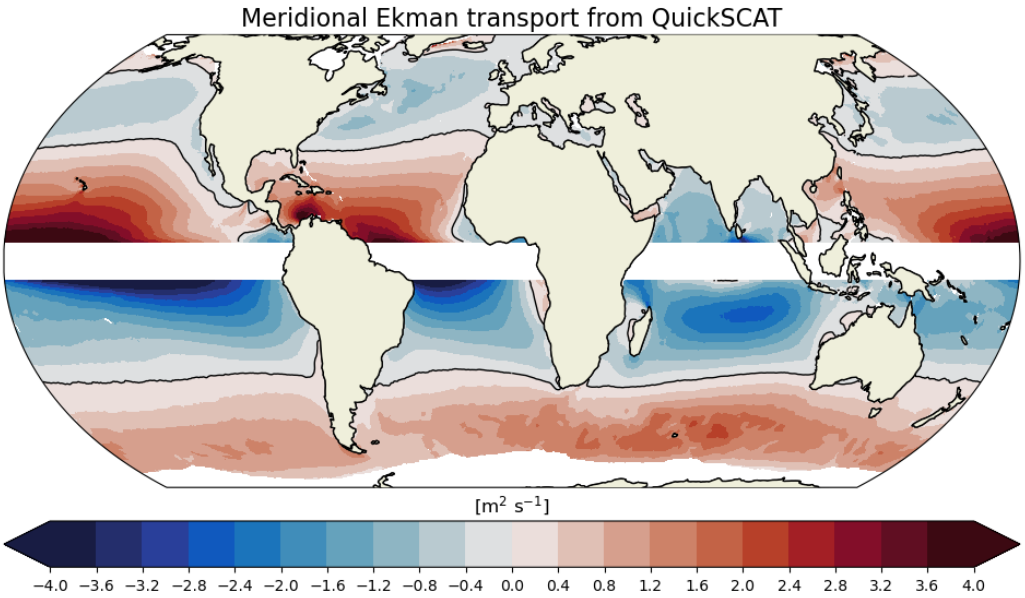

Figure 4.8: *Meridional Ekman volume transport, $-\tau^x / (f\rho_0)$, from QuickSCAT.*

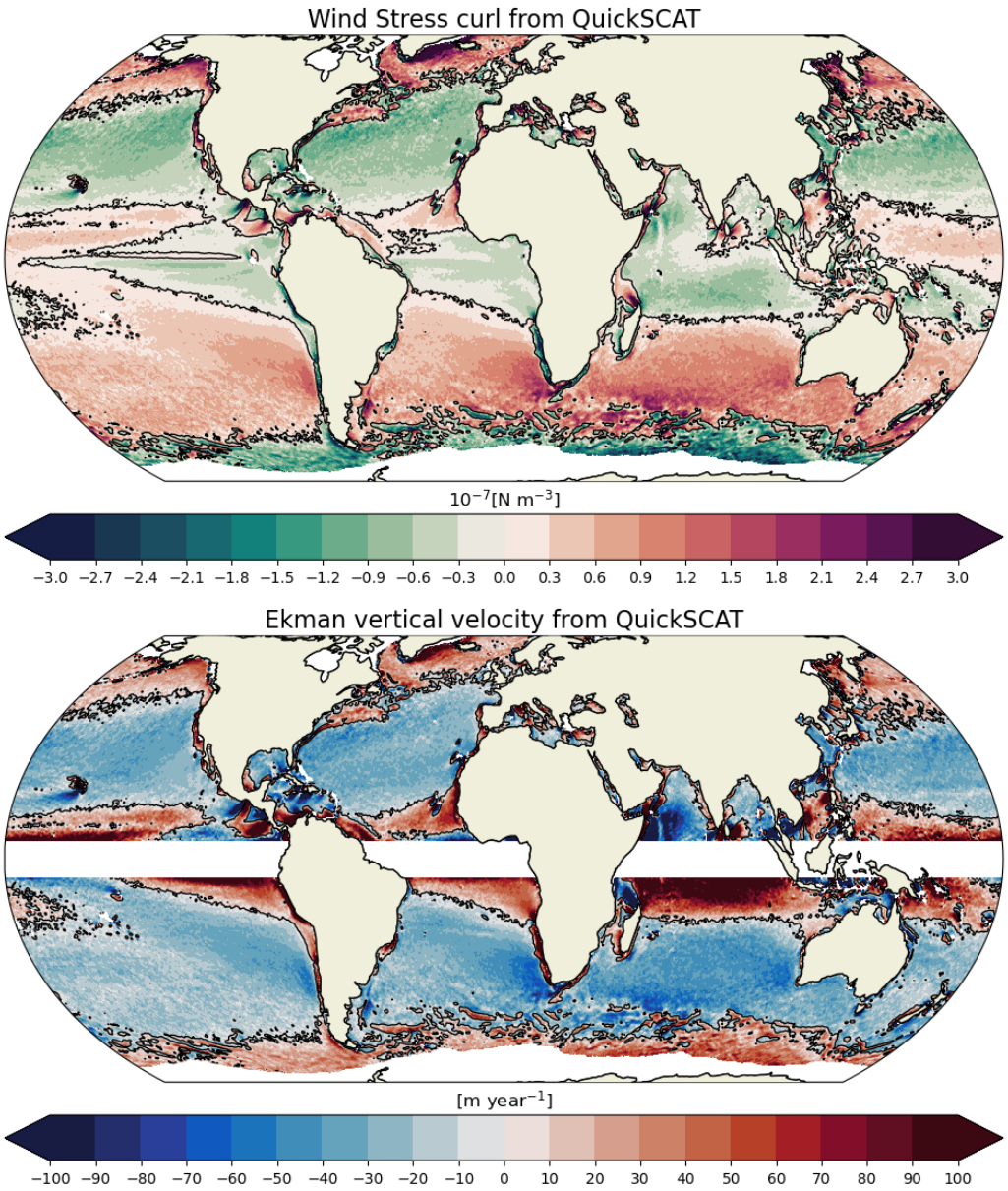

Figure 4.9: *Climatological wind stress curl and Ekman pumping velocity, w_e (m/year), from QuickSCAT. It is negative in the subtropical regions on the order of 20-50 m per year and mostly positive over the subpolar regions. Towards the equator, f goes to zero, and Ekman pumping and Ekman transport become ill-defined.*

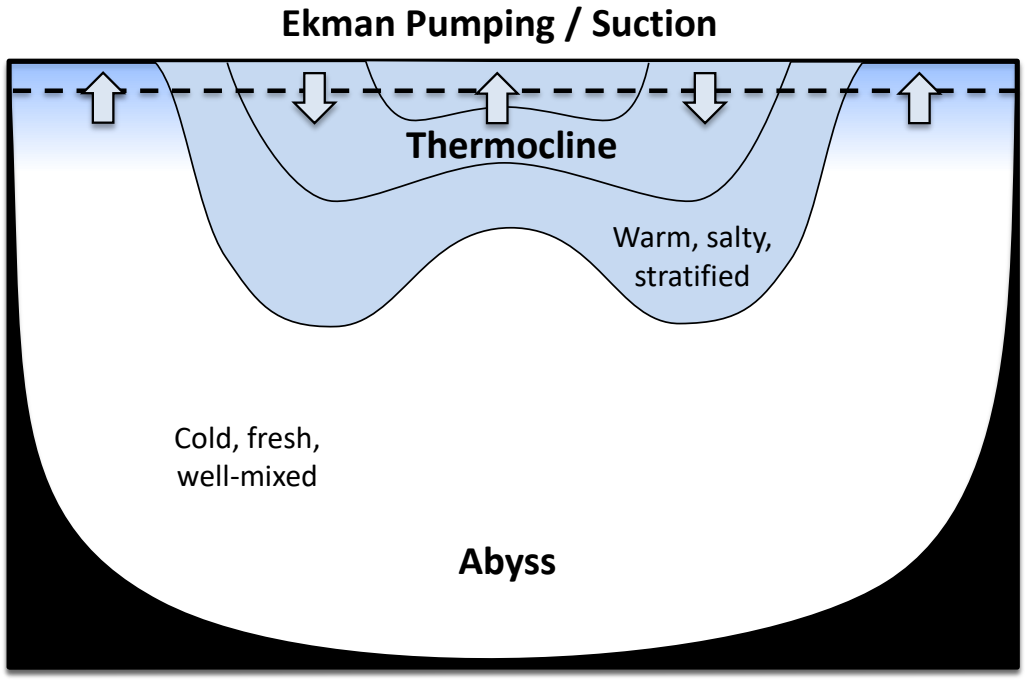

Figure 4.10: *The direction of Ekman pumping and suction is responsible for the odd bi-modal shape of the ocean's density anomaly.*

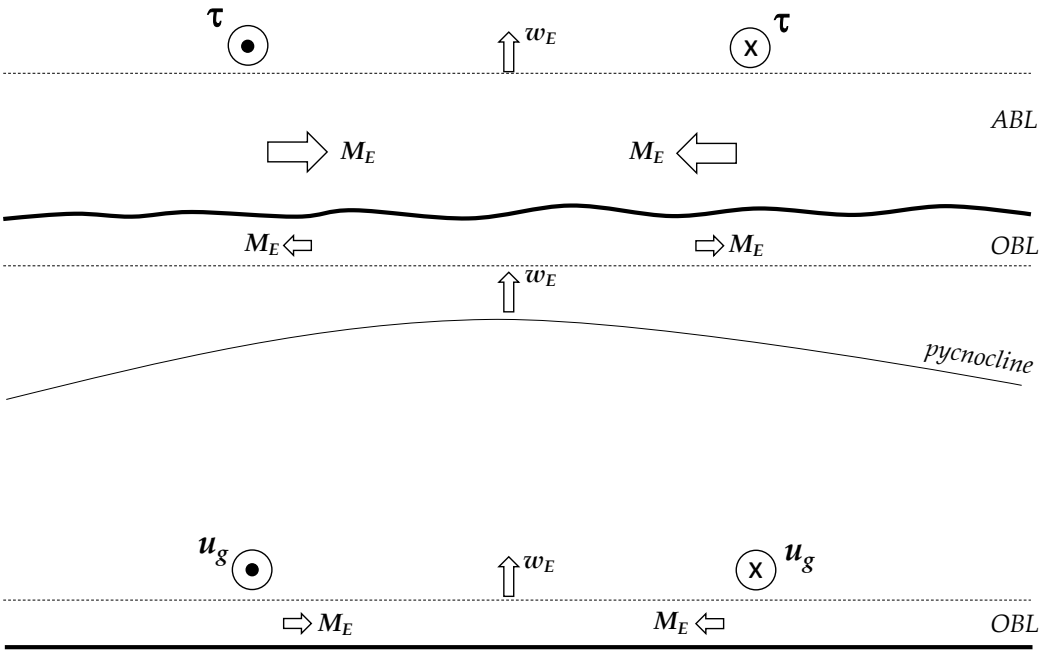

Figure 4.11: *Section through a cyclonic wind over the ocean. The geostrophic wind gives a cyclonic rotation around the low-pressure center. The Ekman mass transport in the atmospheric boundary layer is inward, bringing mass to fill the low, and the associated vertical pumping velocity is therefore upward. The Ekman mass transport in the oceanic boundary layer is equal and opposite to that in the atmosphere, so there is an outward mass transport and upward pumping velocity in the ocean. This tends to raise the thermocline. The upper Ekman layer in the ocean is primarily driven by an imposed wind stress, whereas the lower Ekman layer in the ocean largely results from the interaction of interior geostrophic velocity and a rigid lower surface [from* **?** *and* **?***].*

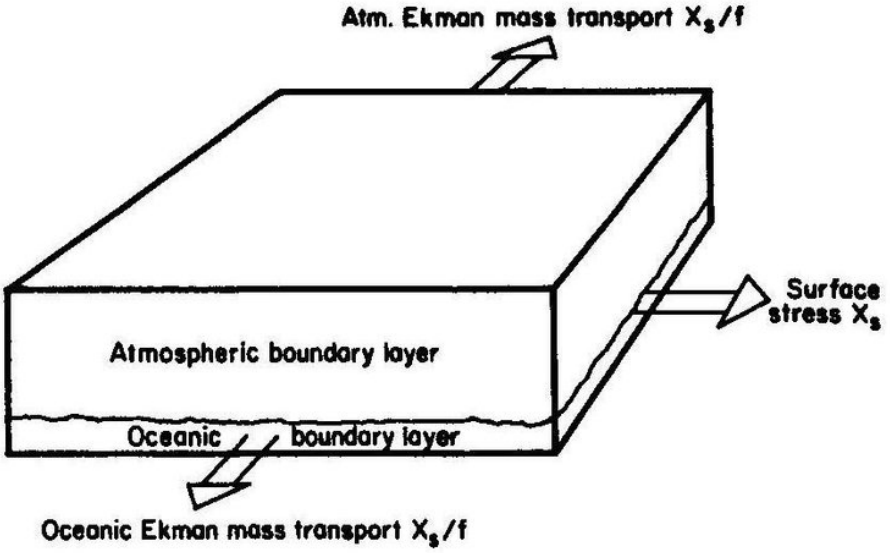

Figure 4.12: *The directions, for the northern hemisphere, and magnitude of the steady Ekman mass transports in the atmosphere and oceanic boundary layers when stress at the surface has the direction shown. Note that the sum of the atmospheric and oceanic Ekman mass transports is zero. When there is no pressure gradient, the force per unit area exerted by the surface stress on each boundary layer is equal to the product of mass per unit area and the Coriolis acceleration of the layer. The latter quantity is f times the Ekman mass transport and is directed at right angles to the stress. [from* **?***]*

Ekman velocity Spiral

- Frictionally induced surface velocity to the right of the wind (for $f > 0$, due to Coriolis)
- Surface layer pushes next layer down slightly to the right, generating a slightly weaker current
- Next layer pushes next layer, slightly to right and generating a slightly weaker current
- Producing a "spiral" of the current vectors, to the right in the northern hemisphere, with decreasing speed as depth increases
- Details of the spiral depend on the vertical viscosity (how frictional the flow is, and also whether friction depends on depth)
- The total transport only depends on the imposed wind stress
- Typical transport size: for a wind stress 0.1 N m^{-2}, $M_E = \tau/(\rho f)$ =1 m^2 s^{-1}. Integrate this over 'width' of the ocean, say 5000 km, we get a total transport of 5×10^6 m^3 s^{-1}= 5 Sv (1 $Sv \equiv 10^6$ m^3 s^{-1})

4.5 Upwelling

4.5.1 Coastal Upwelling

Suppose we have a wind which is entirely meridional, $\tau^x = 0$, and therefore $M_E^y = 0$ and $M_E^x > 0$ for $\tau^y > 0$. The net transport will be to the left of and at right angles to the wind direction (for $f < 0$). Continuity requires that there must be inflow from the right of the wind direction. If the wind is blowing parallel to a coastline which is on the right of the wind, as the wind causes an Ekman frictionally induced transport to the left away from the coast, water is replaced from below, generating a so-called *coastal upwelling* near the region of divergence along the coast.

Coastal upwelling is accompanied by a rise in upper ocean isopycnals toward the coast. This creates an equatorward geostrophic surface flow, the *eastern boundary current*. Poleward undercurrents are observed at about 200 m depth beneath the equatorward surface currents (Fig.4.13c). Poleward undercurrents are created mainly by the alongshore pressure gradient that drives the onshore subsurface geostrophic flow that feeds the upwelling.

Given the prevailing wind directions, the largest coastal upwelling regions happen to be on eastern boundaries of ocean basins. Eastern boundary upwelling systems (EBUS) cover less than 3% of the world ocean surface yet they have a significant role in the climate system, and are home to the largest contribution of ocean biological productivity with up to 40% of the reported global fish catch (Fig.4.14). The upwelled water does not come from great depths. Observations and models show that upwelled water comes from depths not greater than 200-300 m. Usually the upwelled water has high nutrient content, and plankton production may be promoted with important biological consequences when photosynthesis is activated in the photic zone.

Coupled with the vast coastal human populations, these regions play key biological and socio-economical roles. There are common features to eastern boundary upwelling regions: wind-driven flows, alongshore currents, steep shelves and large vertical and offshore nutrient transports. Despite the commonality, each of the main upwelling systems (California, Humboldt, Canary and Benguela Current Systems), exhibits substantial differences in primary productivity, phytoplankton biomass, and community structures. The reasons for these differences are not fully understood.

Many coupled climate models generate very large sea surface temperature (SST) biases in the coastal upwelling regions of the California Current System, the Humboldt Current system and the Benguela Current System,

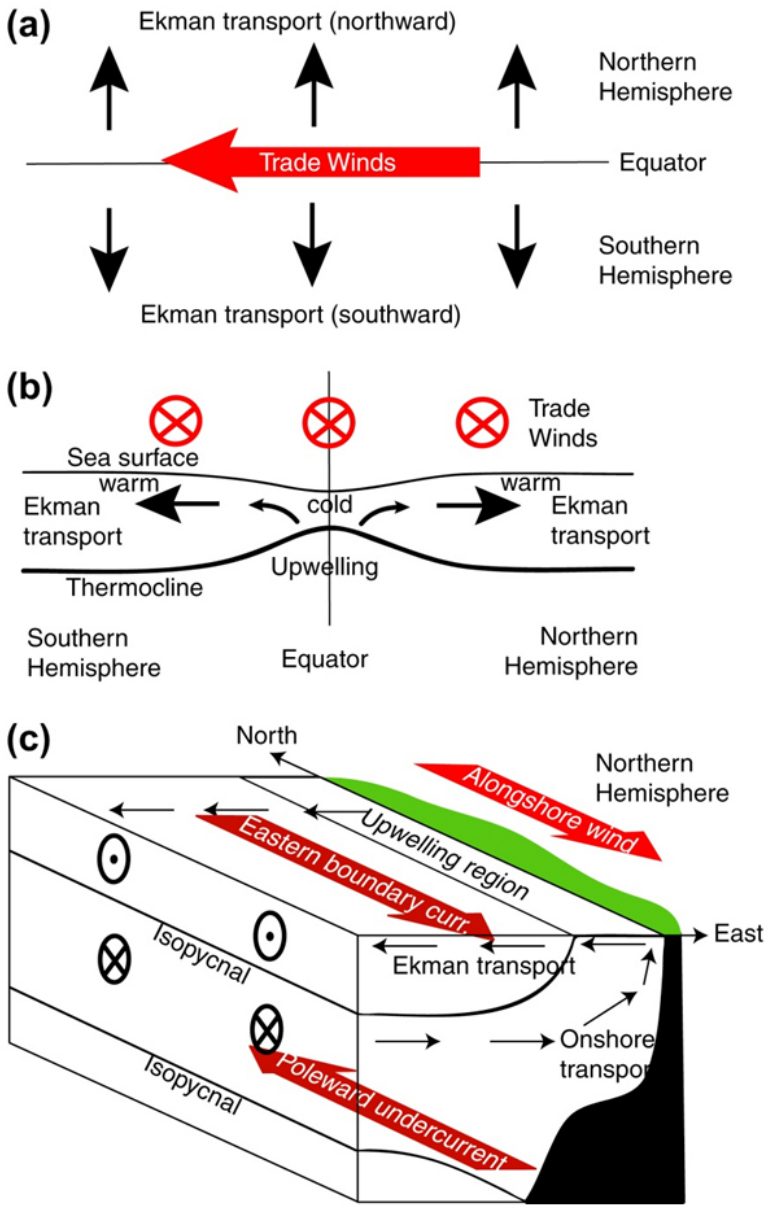

Figure 4.13: *Ekman transport divergence near the equator driven by easterly trade winds. (a) Ekman transports. (b) Meridional cross-section showing effect on the thermocline and surface temperature. (c) Coastal upwelling system due to an alongshore wind with offshore Ekman transport ($f > 0$). The accompanying isopycnal deformations and equatorward eastern boundary current and poleward undercurrent are also shown. [from* **?***]*

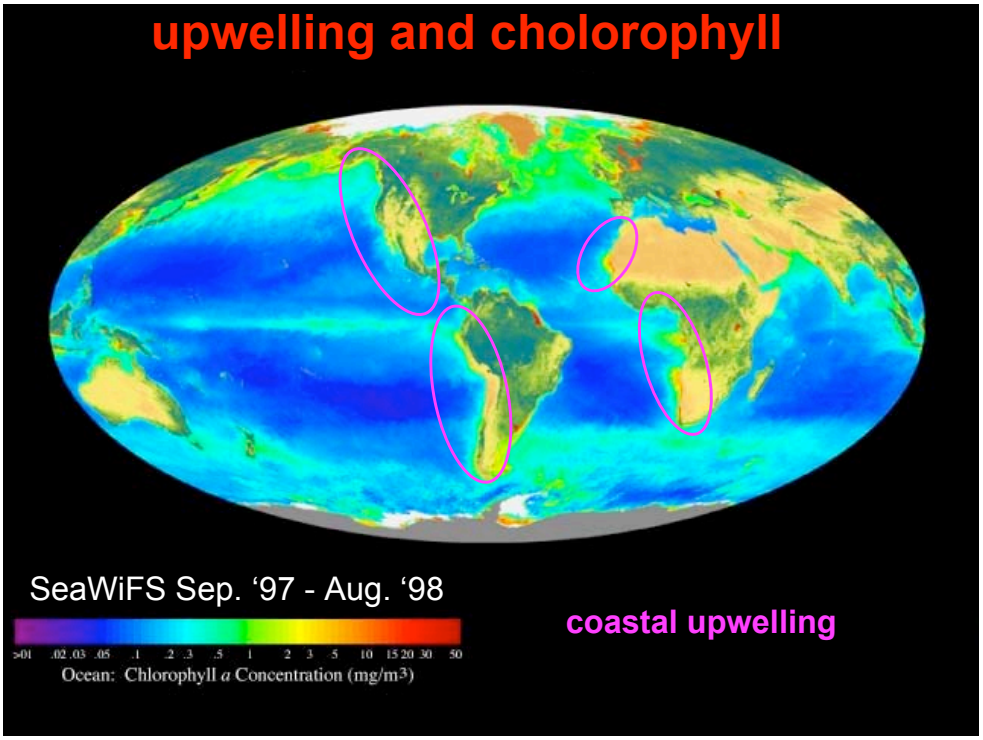

Figure 4.14: *A false-color image depicting chlorophyll-a concentration as measured from the SeaWIFS satellite data. Eastern Boundary Upwelling systems (EBUS) regions (California, Peru, Canary and Benguela) are shown by the pink ovals.*

where simulated mean SSTs are much warmer than observed (typically in excess of 3°C and as high as 10°C; see Fig.4.16). Furthermore, these SST biases have significant remote effects on surface and subsurface temperature and salinity, and on precipitation and hence atmospheric heating and circulation. The warm temperature biases associated with upwelling regions strongly limit the prediction of future evolution of these regions. Increased model resolution, achieved via nesting or adaptive gridding, improves simulations of the regional climate and affects the large-scale climate system through feedbacks.

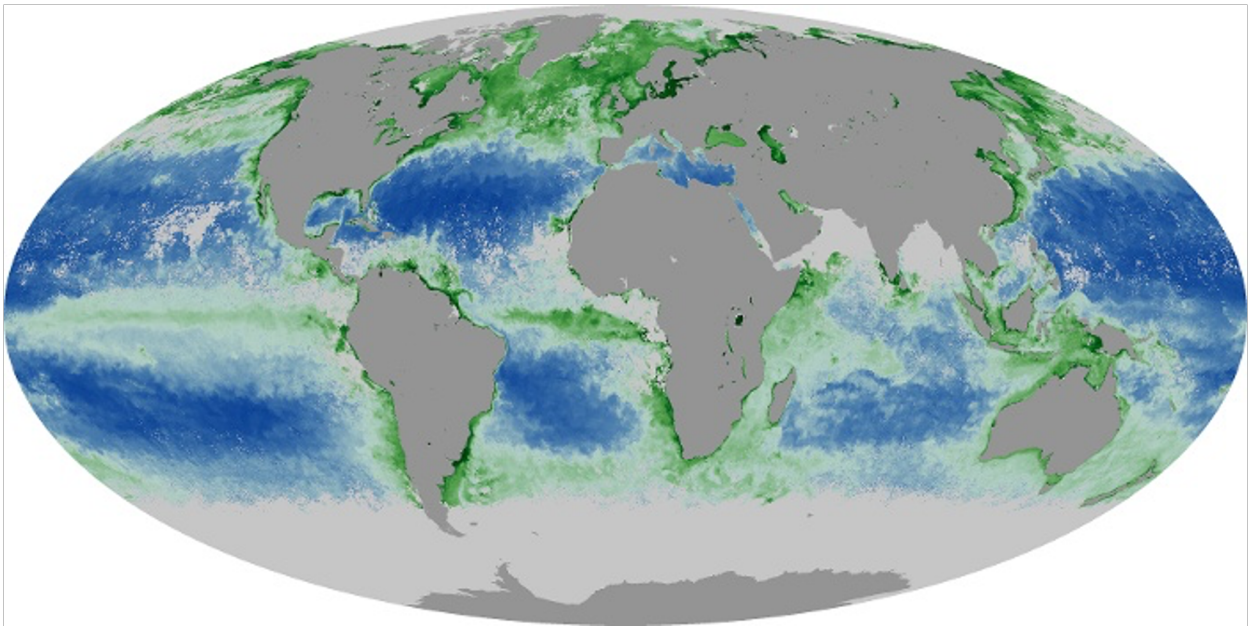

Figure 4.15: *Same as in Fig.4.14. Can you see dynamics here?*

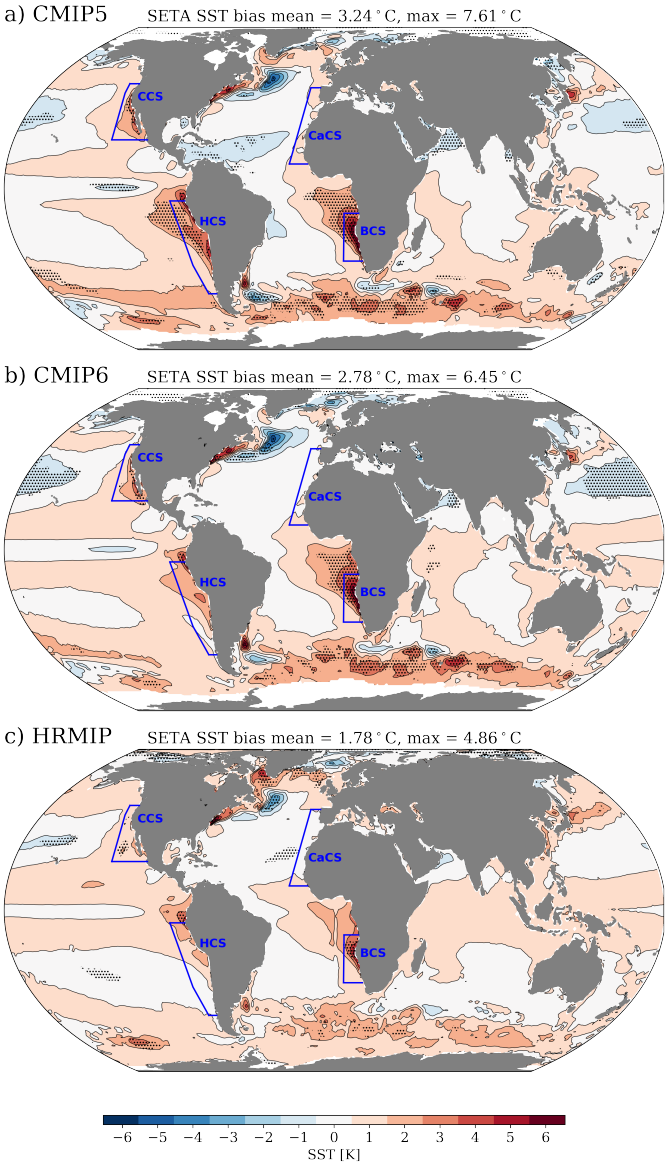

Figure 4.16: *Time-mean (1985-2004) SST bias for (a) CMIP5, (b) CMIP6 and (c) HighResMIP multi-model mean relative to OISST. Every contour represents an SST bias of 1 K. Black dots show regions where all models agree on the sign of the bias. The poles are excluded in order to highlight the biases in the EBUS regions, which present the highest SST anomalies. The 4 major EBUS are: the California Current System (CCS), the Canary Current System (CaCS), the Humboldt Current system (HCS) and the Benguela Current System (BCS). [from* **?***]*

4.5.2 Equatorial Upwelling

Equatorial upwelling due to Ekman transport results from the westward wind stress (trade winds). These cause northward Ekman transport north of the equator and southward Ekman transport south of the equator. This results in upwelling along the equator, even though the wind stress curl is small because of the Coriolis parameter dependence in (4.33).

At the equator, where the Coriolis parameter changes sign, zonal (east-west) winds can cause Ekman convergence or divergence even without any variation in the wind (Fig.4.13a). Right on the equator, there is no Ekman layer since the Coriolis force that would create it is zero ($f = 0$). If the equatorial wind is westward (a trade wind), then the Ekman transport just north of the equator is northward, and the Ekman transport just south of the equator is southward, and there must be upwelling into the surface layer on the equator.

Trade winds are relatively steady easterlies. They are driven by warm waters in the western region and cooler waters in the east, which creates rising air in the west and sinking air in the east, and a thermally direct flow from east to west to feed this (Walker cell). In the ocean the true equatorial region is much narrower - about 2 degrees wide. Easterly trade winds at the equator drive (1) poleward Ekman transport and (2) westward surface flow, as follows. The easterly trade winds cause northward Ekman transport just to the north of the equator and southward Ekman transport just to the south of the equator. This causes upwelling at the equator. As a result, the pycnocline shoals towards the equator (Fig.4.13b). **This drives a westward geostrophic flow at the sea surface.**

Directly on the equator, the effect of rotation on the circulation vanishes, and so the concepts of geostrophic and Ekman flow do not apply. At the equator, the easterly trade winds push the surface water directly (frictionally) from east to west. This water piles up gently in the western Pacific (0.5 meters higher there than in the eastern Pacific). The pycnocline is deeper in the west also as a result, and much warmer water is found there (so-called **"warm pool"**). Upwelling in the east draws cool water to the surface because of the shallow pycnocline there, but intense eastward-flowing upwelling in the west cannot create cold water at the surface there because of the thickness of the warm pool.

Because the sea surface is higher in the west than in the east, there is a pressure difference that causes the flow just beneath the surface layer to be eastward. This strong eastward flow is the Equatorial Undercurrent. It is centered at about 150 to 200 m depth. EUC speeds are in excess of 100 cm/sec. The current is exceptionally thin vertically (about 150 m

thick). The Equatorial Undercurrent shoals towards the east, as does the pycnocline. The shoaling is associated with upwelling of cool water in the central/eastern Pacific, giving rise to the ”cold tongue” (in non-El Niño years). Steady trade winds, which cause equatorial upwelling, are more prevalent in the east than in the west. When the trade winds weaken or even reverse, the flow of water westward at the equator weakens or reverses and upwelling weakens or stops. Surface waters in the eastern Pacific warm significantly since upwelling is no longer bringing the cool waters to the surface. The deep warm pool in the western Pacific thins as its water sloshes eastward along the equator in the absence of the trade winds which maintain it.

Exercices

1. For $A = 10^{-1}$ m^2 s^{-1} and $f = 10^{-4}\ s^{-1}$, what would be the typical depth of an Ekman layer?

2. Assume that the atmospheric Ekman layer over the earth's surface at latitude 45°N can be modeled with a turbulent kinematic viscosity $\nu = 10$m^2 s^{-1}. If the geostrophic velocity above the layer is 10 m s^{-1} and is uniform, what is the vertically integrated flow across the isobars (pressure contours)? Is there any vertical velocity?

3. Meteorological observations above New York City (41°N) reveal a neutral atmospheric boundary layer (no convection and no stratification) and a westerly geostrophic wind of 12 m s^{-1} at 1000 m above street level. Under neutral conditions, Ekman layer dynamics apply. Using an eddy viscosity of 10 m^2 s^{-1}, determine the wind speed and direction atop the World Trade Center (height: 411 m).

4. Between 15°N and 45°N, the winds over the North Pacific consist mostly of the easterly trades (15°N to 30°N) and the westerlies (30°N to 45°N. An adequate representation is

$$\tau^x = \tau_0 sin\Big(\frac{\pi y}{2L}\Big), \quad \tau^y = 0, \quad -L \leq y \leq L, \tag{4.95}$$

   where $\tau_0 = 0.15\ N/m^2$ is the maximum wind stress and $L = 1670\ km$. Taking $\rho_0 = 1028\ kg/m^3$ and the value of the Coriolis parameter corresponding to 30°N, calculate the Ekman pumping. Which way is it directed? Calculate the vertical volume flux over the entire 15°N-45°N strip of the North Pacific (width = 8700 km). Express your answer in Sverdrup units (1 Sverdrup = 1 Sv $\equiv 10^6$ m^3 s^{-1}).